SUPER-RESOLVED PARAMETERIZATION OF DISPERSIVE SCATTERING MECHANISMS IN THE TIME-FREQUENCY PLANE

Luiz C. Trintinalia* and Hao Ling
Department of Electrical and Computer Engineering
The University of Texas at Austin
Austin, Texas 78712-1084

1 - Introduction

Time-frequency techniques such as the short-time Fourier transform (STFT) and wavelet analysis have been recently used to process wideband radar echo from complex targets [1-4]. In the two-dimensional time-frequency plane, scattering centers, target resonances and dispersive phenomena can be simultaneously displayed. However the additional insights gained in the time-frequency plane come at the cost of loss of resolution. Recently Moore and Ling [5] proposed a windowed super-resolution procedure that would allow the parameterization of both scattering centers and resonances present in wideband backscattered signals. However, that procedure could not handle data containing dispersive mechanisms.

In this paper we implement a super-resolution algorithm that allows the full parameterization of waveguide-type dispersion mechanisms. In our algorithm, ESPRIT [6] is used as the processing engine. Since super-resolution methods in their original form are not equipped to handle dispersive behaviors, additional processing is required to parameterize the data. We use ESPRIT both in the time and frequency domain to extract the cutoff frequencies and the delays associated with each mode. A nonlinear sampling scheme is then used to come up with an improved estimate of the cutoff frequencies. Finally, a polynomial fit for the amplitude of each mode is performed to fully parameterize the data. The resulting curves can be displayed in the time-frequency plane with very high resolution.

2 - Description of the Method

In this work we focus on phenomena related to the propagation of waves in exposed waveguide structures such as open-ended ducts and slotted waveguides. The dispersive behavior exhibited by these structures is due to energy that propagates in the form of waveguide modes. Therefore signals of the form:

$$E(f) = \sum_n A_n e^{-j2\pi\sqrt{f^2-f_{cn}^2}\,\tau_n} e^{-j2\pi f t_n} \quad (1)$$

are expected. In this expression, f_{cn} is the cutoff frequency of the mode, τ_n is equal to the length of the guided path for this signal component divided by the speed of light and t_n is some other additional delay due to non-dispersive propagation paths. The amplitude of each of these components, A_n, is also allowed to be a slowly varying function of frequency. Note that in the limit as f_{cn} approaches zero, the above expression reduces to the standard scattering center model.

The objective of this work is to extract all the unknown parameters in (1), for each of the components present in the scattered signal, from the backscattered data. To achieve this, we first obtain the time-domain representation $e(t)$ of (1) using the inverse discrete Fourier transform (IDFT). It can be shown that each component will tend towards a complex sinusoid of frequency f_{cn} during the late time. Therefore we can extract a first approximation for the cutoff frequencies from the late-time data. Once the estimates for the cutoff frequencies are in hand, we can extract the non-dispersive scattering centers from the data. We apply ESPRIT, but now in the frequency domain, using only the frequencies below the first cutoff. The respective amplitudes can be obtained by a polynomial approximation and a simple least square estimate.

If all the remaining components are related to the same waveguide path, they will have the same delays τ_n and t_n, but with different cutoff frequencies. To find these delays we can examine the group delay of a single mode:

$$t_{gn} = \frac{-1}{2\pi}\frac{\partial \Phi_n}{\partial f} = t_n + \frac{\tau_n f}{\sqrt{f^2 - f_{cn}^2}} \quad (2)$$

By sliding a small window in the frequency domain between the first and the second cutoff frequencies, and applying ESPRIT for each position of this window, we can extract an approximation for the group delay for different frequencies. Fitting expression (2) to the resulting data (which is just a linear least square estimate problem) we obtain the estimates for τ_n and t_n.

In the last step, we eliminate the linear delay from the expression (1) by multiplying our data by $e^{j2\pi f t_n}$, still assuming that all the components have the same delay. We obtain:

$$E'(f) = \sum_n A_n e^{-j2\pi\sqrt{f^2 - f_{cn}^2}\,\tau} \quad (3)$$

In the time domain this expression can be written as:

$$e'(t) = \sum_n B_n\left(\sqrt{t^2 - \tau^2}\right) e^{j2\pi f_{cn}\sqrt{t^2-\tau^2}} u(t-\tau) \quad (4)$$

By the change of variable $x = \sqrt{t^2 - \tau^2}$, we see that expression (4) is just a summation of sinusoids of frequencies f_{cn}. Therefore, we can apply ESPRIT in the x domain to extract new estimates of f_{cn}. We compute $e(x)$ using a nonlinearly sampled IDFT. Now, the amplitudes A_n can be obtained by polynomial approximation and a simple least square estimate.

Finally we can iterate the above procedure to improve the accuracy in the results. Also, a nonlinear optimization of the values for the delays may be used. Since the estimated values are very close to the optimal ones, this final fine tuning is quick and easy.

3 - Results

The algorithm described above was applied to the backscattered data from an open-ended circular waveguide with a diameter of 4.445 cm. A flat conducting termination exists 60.96 cm inside the waveguide (Fig. 1). This data was generated in the frequency domain, taking into account the interior cavity contribution using a modal approach and the diffraction from the front rim of the cavity using an asymptotic formula [7]. The numerical simulation was performed from 2 to 18 GHz in 0.0313 GHz steps. The time-frequency representation for this geometry has already been presented in [1] and [2]. Fig. 3 shows the STFT of the simulated data.

In Fig. 2 we see the comparison between the simulated frequency domain data and the parameterized one. The discrepancy between these two is just 5.35 % of the total energy, with a very good agreement between the extracted cutoff frequencies and the expected values. Fig. 4 shows the super-resolved time-frequency representation we have obtained using our super-resolution procedure. It clearly shows the positions of the scattering center and the modal dispersions as given in equation (2). The intensity at each point is depicted by a gray scale strength. We can see that the curves plotted in this figure give a much clearer and more precise visualization of the phenomena involved when compared to the STFT image of Fig. 3.

4 - Acknowledgments

This work was support by the Joint Services Electronics Program under Contract No. AFSOR F49620-92-C-0027. L. C. T. is on leave from the Department of Electronic Engineering of Escola Politécnica da Universidade de São Paulo, Brazil and is also sponsored by CNPq.

5 - References

[1] H. Ling and H. Kim, "Wavelet analysis of backscattered data from an open-ended waveguide cavity," *IEEE Microwave and Guided Wave Lett.*, vol. 2, pp. 140-142, Apr. 1992.

[2] A. Moghaddar and E. K. Walton, "Time-frequency-distribution analysis of scattering from waveguide cavities," *IEEE Trans. Antennas Propagat.*, vol. AP-41, pp. 677-680, May 1993.

[3] H. Ling, J. Moore, D. Bouche and V. Saavedra, "Time-frequency analysis of backscattered data from a coated strip with a gap," *IEEE Trans. Antennas Propagat.*, vol. AP-41, pp. 1147-1150, Aug. 1993.

[4] L. Carin, L. B. Felsen, D. Kralj, S. U. Pillai and W. C. Lee, "Dispersive modes in the time domain: analysis and time-frequency representation," *IEEE Microwave Guided Wave Lett.*, vol. 4, pp. 23-25, Jan. 1994.

[5] J. Moore and H. Ling, "Super-resolved time-frequency analysis of wideband backscattered data," accepted for publication in *IEEE Trans. Antennas Propagat.*

[6] R. Roy, A. Paulraj, and T. Kailath, "ESPRIT - a subspace rotation approach to estimation of parameters of cisoids in noise", *IEEE Trans. Acoustics Speech Sig. Proc.*, vol. ASSP-34, pp. 1340-1342, Oct. 1986.

[7] H. Ling, S. W. Lee, and R. Chou, "High-frequency RCS of open cavities with rectangular and circular cross sections," *IEEE Trans. Antennas Propagat.*, vol. AP-37, pp. 648-654, May 1989.

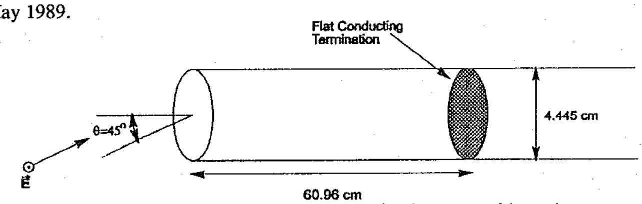

Fig. 1. Geometry of the open-ended circular waveguide cavity

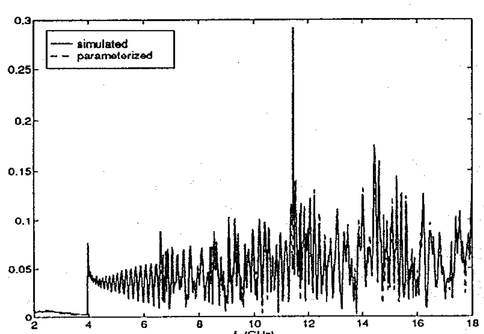

Fig. 2. Comparison between simulated data and parameterized data.

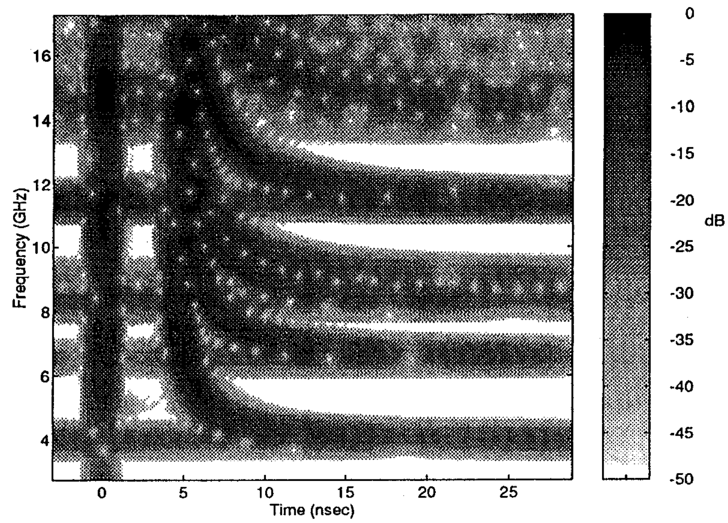

Fig. 3. STFT of simulated data.

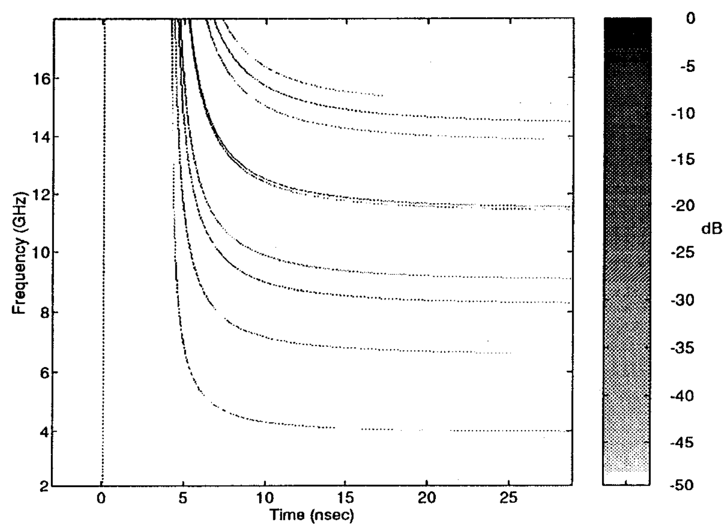

Fig. 4. Super-resolved time-frequency display.